Determination of chlorpheniramine maleate in its pharmaceutical preparations using homemade turbidity flow injection analyzer

*Muntadhar M. Jabbar**[ID][✉], *Elham N. Mezaal*[ID][✉]

Department of Chemistry, College of Education for Pure Science (Ibn Al-Haitham), University of Baghdad, Baghdad, Iraq.
*Corresponding Author.

Abstract

By using continuous flow injection analysis technology, a new analytical method was presented for the determination of chlorpheniramine maleate (CPM) in its pure form and in some of its pharmaceutical preparations. The study was based on the reaction of CPM with ammonium ceric(IV) sulphate (ACS) in an acidic medium, where the reaction resulted in a slightly yellowish white precipitate. It was studied using Ayah 6S×1-ST-2D solar cell CFI analyzer (homemade) by measuring the light reflected from the surfaces of precipitate particles at $(0-180^0)$. Several experiments were conducted to study and improve the chemical and physical parameters. The correlation coefficient (r) = 0.9996, and the linear calibration curve was within the range (0.07-5mmol/L). The detection limit (L.O.D) was 195ng/10µL. The relative percentage deviation RSD% was less than 0.2% for the concentration of 1.0, 1.5 and 4.0mmol/L of CPM for n= 8. The method was successfully applied in estimating CPM in three samples of pharmaceutical preparations available in the Iraqi pharmaceutical market for three different companies. The new method was compared with the UV–Vis spectrophotometric method at λ_{max}= 261nm. To ensure that there was no significant difference between the proposed method and the spectrophotometric method, both a t-test and a F-test were conducted. The results of the two tests showed that there was no significant difference at the 95% confidence level, where the t-result was calculated (|-2.162). It is less than the t-tabular value (4.303) and also the calculated F value (31.9770) is less than the tabular F value

Keywords: Antihistamines, chloropheniramine malate, CFI Analyzer, continuous flow injection, precipitate particles, UV-Vis spectrophotometric method.

Introduction

Chlorpheniramine maleate (CPM): [(3-(4-chlorophenyl)-N,N-dimethyl-3-pyridin-2-yl-propane-1-amine], chemical formula $C_{16}H_{19}ClN_2.C_4H_4O_4$, chemical structure as in Fig. 1, is white, odorless, crystalline powder, bitter in taste, soluble in alcohol and chloroform, as well as being freely soluble in water and slightly soluble in ether and benzene [1-3]. The release of histamine and other substances that cause allergy symptoms [4-7] that come as a defensive reaction of the immune system, it requires the use of medications called antihistamines [8-11], including CPM, which is used to reduce allergy symptoms such as watery eyes, itchy eyes, skin irritation, itching caused by insect bites, and other conditions such as chickenpox, measles, and to treat colds and conjunctivitis [12-15].

The H1 histamine receptor mechanism is where chlorpheniramine binds. The effects of endogenous histamine are blocked by CPM, temporarily alleviating histamine-induced symptoms [16-18]. Common side effects of CPM include drowsiness, insomnia, weakness and dry mouth [19-21].

Several methods have been developed to determine CPM, some of which are but not limited to: spectroscopic methods [22-24], HPLC [25-27], RP-HPLC [28-31], gas chromatography [32], flow injection methods [33]. However, these analytical methods have some disadvantages such as due to the lack of modeling, that is, it requires a long time to analyze a large number of samples, and some of them make extensive use of toxic solvents, in addition to their need for expensive devices, equipment, and maintenance. Since resources and equipment such as HPLC are not available in many laboratories, it is necessary to develop a method that is easy to implement using readily available equipment. To achieve this purpose, a new method was proposed within the continuous flow injection analysis technique [34-36] using homemade cells [37, 38], which are based on turbidity measurement[39-42], which could be an alternative to the commonly used UV-Vis spectrophotometric method. It was done using a CFI analyzer for homemade solar cells (Ayah 6SX1-ST-2D solar cell CFI analyzer) [43], which has been used

by many researchers. In the identification of some drugs [44, 45]. The study aims to present a fast, easy-to-work, environmentally friendly, low-cost, reproducible and high-recovery analytical method for CPM that is low in pollution and safe because the reaction occurs in a closed system. In addition, it meets part of the requirements of green chemistry[46], as the solvent used in all study experiments is distilled water, which is classified as a green solvent.
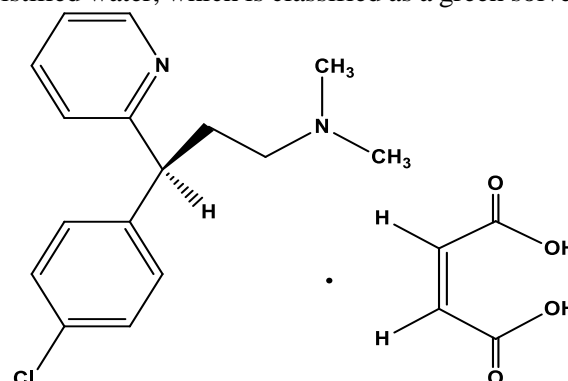

Figure 1. Chemical structure of CPM.

Materials and Methods

Reagents and chemicals

All chemicals were of analytical-reagent grade while distilled water was used to prepare the solution. The standard solution (10mmol/L) of the CPM (supplied from SDI, 390.86g/mol) was prepared by taking 0.39086 g and dissolving it in 100ml of distilled water. The standard solution of ACS (supplied from Hopkin & Williams, 659.62 g/mol) was prepared by taking 6.5962 g of it and dissolving it in 500 ml of distilled water to obtain a concentration of 20 mmol/L. While 100 mmol/L of each of the following acids was used (supplied from BDH): H_2SO_4 (98% w/w, 1.84 g/mol) , HCl (35% w/w, 1.19 g/ml), HNO_3 (70% w/w, 1.42 g/mol), CH_3COOH (99.5% w/w , 1.05g/mol). While 100 mmol/L of each of the following salt solutions was used (supplied from BDH): NaCl (58.44 g/mol), $NaNO_2$(68.9953 g/mol), $NaNO_3$ (84.9947 g/mol), NH_4Cl (53.491 g/mol), Na_2CO_3 (105.99 g/mol) and the washing buffer solution was prepared by dissolving 40 g of ethylene diamine tetra acetic acid (EDTA) and 7 g of ammonium chloride in distilled water, then adding 57 ml of 25% (V/V) ammonia. The volume was completed to the mark in a 1L volumetric flask with distilled water.

Sample preparation

Using a ceramic mortar and pestle, 20 tablets of each pharmaceutical formulation were smashed, and they were then sorted through a 200-mesh sieve. In order to obtain 10 mmol/L, each medication containing 4 mg of CPM (supplied by SDI-Iraq, Julphar-UAE, and Al-Kindi-Iraq) was weighed at 1.1299, 1.0772, and 0.9873 g, on the relay. Distilled water was used to dissolve the powder; the volume was then filled to a total of (10 ml) with distilled water. Followed filtered to remove any undissolved residue that might have affected the responses.

Apparatus

The apparatus used in the new method for CPM determination consists of two-channel variable speed (5-40) peristaltic pump (supplied from Ismatec – Switzerland) and three pairs-hole medium pressure injection valves (It was supplied by IDEX Co.-U.S.A.) with sample loop (0.7 mm i.d. Teflon, different length). Ayah 6S×1-ST-2D Solar cell-CFI Analyzer (Homemade, 6S ×1:Six linearly arranged and adjacent sources of same class and the same irradiation light, which is the snowy white light, ST: Spectral & Turbidity , 2D:Two detectors) it was used to measure the response expressed in mV, three pairs (6) snow white LEDs are used as a beam source in the flow cell (Flow cell of cylindrical tube of glass with I.D 2 mm, O.D of 4 mm of transparent Pyrex

glass of 70 mm length embedded inside a metal black. The flow cell is connected using silicone rubber and Teflon tubes having a different inside diameter) where the path length 2mm. As a detector to collect signals via a 60 mm travel sample, two solar cells (two solar cell act as a direct detector. The dimension 30 mm (length) x 14 mm (width) and 1mm thickness embedded in the metal block) were used[43]. The response is output in the form of peaks

through the x-t potentiometric recorder (Kompenso GraphC-1032, supplied from Siemens-Germany, 1-5 volt, 1-500 mV), the flow diagram for the determination of CPM shown in Fig. 2. For measurements the UV-Spectrophotometric method was used UV-Vis spectrophotometer (Shimadzu double beam. It wavelengths scan range 190-1100 nm, the measuring cell is 1 ml (1000µl) made of quartz, model UV-1800 Kyoto-Japan).
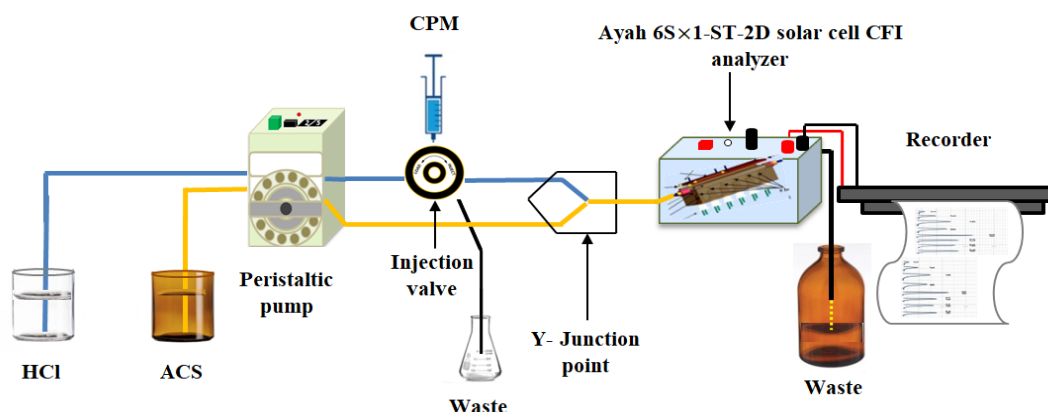

Figure 2. Graphical diagram of the flow system used in the determination of CPM.

Methodology

The manifold flow system which is used for the determination of CPM consisting of two lines which were used to conduct this work as shown in Fig. 2. The determination of CPM was carried out by the reaction between CPM and ACS 16 mmol/L in acidic medium to form a white slightly yellowish precipitate . The first line represents the carrier stream (hydrochloric acid) at 2.0 ml/min flow rate which leads to the injection valve to carry a sample volume 25 µl(experimental) of CPM uses open valve mode, while the second line supplies ACS solution at 2.0 ml/min. Both lines met at a Y-junction, with an outlet for reactants product from

complex, which passes through a homemade Ayah 6SX1-ST-2D solar cell CFI Analyzer. The response profile was recorded on x-t potentiometric recorder to measure energy transducer response expressed as peak heights in mV, where the responses appeared in the form of peaks expressing the response of the transducer and the peak height expressing the amount of light reflected after it fell on the surface of the precipitate particles in the flow cell (that is, the surfaces of the precipitate particles act as a light-reflecting mirror). A proposed mechanism of oxidation of CPM by ACS in an acidic reaction medium is present in scheme 1[47].
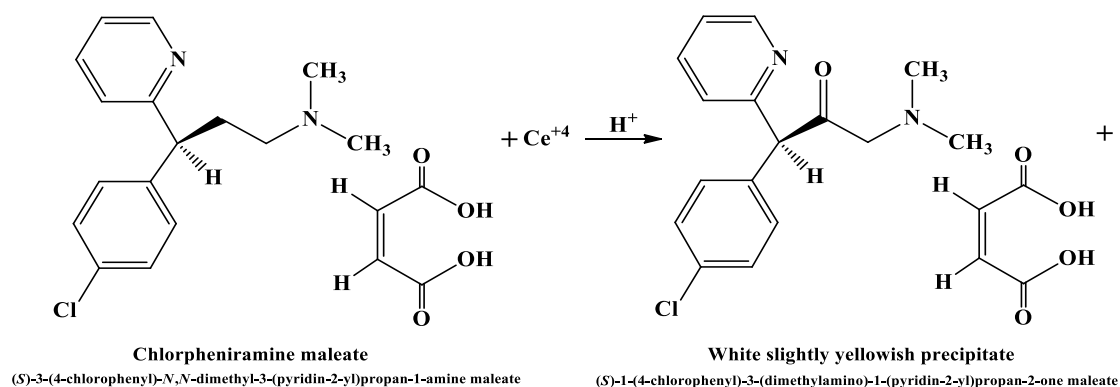
Scheme 1. Proposed reaction between CPM and ACS in acidic medium[47].

Results and Discussion

To determine some optimal parameters, the effect of reagent concentration and the type of reaction medium were studied as chemical parameters, while the effect of flow rate, sample volume, and purge time were studied as physical parameters by changing one parameter and making the other constant each time.

Chemical variables
Effect of ACS concentration

To study the effect of ACS concentration, a series of solutions were prepared with different concentrations within the range (4-20 mmol/L) to reach the optimal concentration and choose it in subsequent experiments. 4 mmol/L of CPM was injected using a sample volume of 25μl and using distilled water as the carrier stream, the flow rate for both the reagent and carrier lines was 2.0 ml/min. The measurement for each concentration was repeated three times. Fig. 3 represents the response profile, which showed that the height of the response peak increased progressively with increasing concentration of the reagent until the concentration was reached 16 mmol/L, then it began to decrease after the aforementioned concentration. This may be attributed, according to the mechanism of operation of the homemade solar cell analyzer, to an increase in the amount of precipitate formed, which causes slow movement of its particles and the increased agglomeration of those particles (part of the reflective surface is damaged) and this causes a smaller amount of reflected light to reach the detector and thus a decrease in the height of the response peak[42-45, 48]. From the response profile, it was noted that the response peak was higher and the base width was lower at the concentration of 16 mmol/L, so it was determined as the optimal concentration for the reagent in subsequent experiments. The results are summarized in Table 1
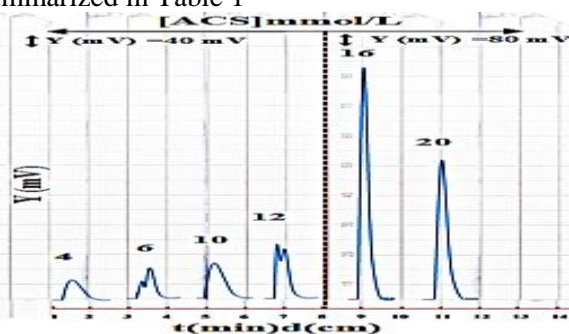

Figure 3. Effect of ACS concentration on response profile versus time.

Table 1. Synopsis of the results of effect of the concentration of ACS reagent on the responses average.

[ACS] mmol/L	Response average $\overline{Y}i(mV)$ for(n=3)	R S D%
4	120	0.2000
6	168	0.2380
10	200	0.2250
12	360	0.2222
16	1576	0.1015
20	752	0.1595

Effect of different medium

To determine the optimal reaction medium between CPM (4 mmol/L) with ACS (16 mmol/L), different solutions were used as carrier current (CH_3COOH, HCl, HNO_3, H_2SO_4, NaCl, NH_4Cl, $NaNO_2$, $NaNO_3$, Na_2CO_3). At a concentration of 100 mmol/L each, in addition to an aqueous medium. The measurement was repeated for each type of mediums three times, and it was found that, with the exception of hydrochloric acid, the various media led to a decrease in the S/N response, Figs. 4 A and B. This may be due to the fact that they caused an increase in the agglomeration of the precipitate particles or the density of the aggregates, which led to them merging with each other and damaging part of the media. From the reflective surface, which causes a smaller amount of reflected light to reach the detector and thus lower response intensity. The higher response shown by the use of hydrochloric acid, as shown in the Fig. 4A, may be attributed to its role in forming precipitate particles that are more numerous and regular (increasing the reflective surface area) and thus increasing the amount of reflected light sent towards the detector. Therefore, it was chosen as an optimal reaction medium in subsequent experiments. The results are summarized in Table 2.
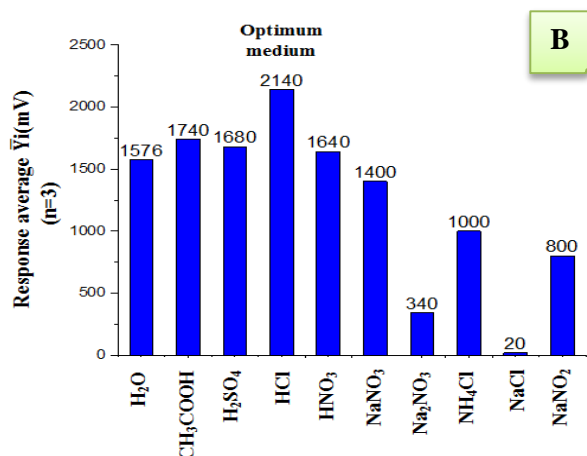

t(min),d(cm)
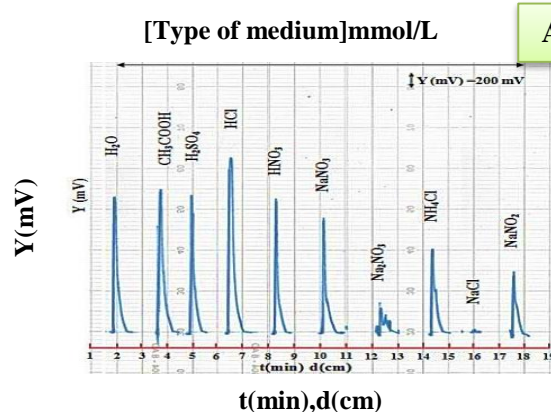
Figure 4. The effects of various medium on: A: response outline versus time. B: Peak rise rate of transducer's response in (mV).

Table 2. A synopsis of the effects of several medium types on the transducer's average responses.

[Type of medium] mmol/L	Response average $\bar{Y}i$(mV) for (n=3)	RSD%
H_2O	1576	0.1015
CH_3COOH	1740	0.1023
H_2SO_4	1680	0.1017
HCl	2140	0.1028
HNO_3	1640	0.1006
$NaNO_3$	1400	0.1071
Na_2CO_3	340	0.1029
NH_4Cl	1000	0.1200
NaCl	20	0.0950
$NaNO_2$	800	0.1025

Effect of HCl concentration

Using the CPM (4 mmol/L)-ACS (16 mmol/L) system, a range of solutions (50-450) mmol/L of hydrochloric acid were prepared using a sample volume of 25 μL and a flow rate of 2.0 mL/min for each line from the first line. (carrier stream) and the second line (reagent stream). The response profile in Fig. 5 showed that the acid concentration of 50 mmol/L gave the highest response and the lowest peak width. This may be attributed to its contribution to the formation of a greater number of precipitate particles (increasing degree above relative saturation). Therefore, 50 mmol/L was chosen as the best concentration for the medium in subsequent experiments. The results of the experiment are summarized in a Table 3.
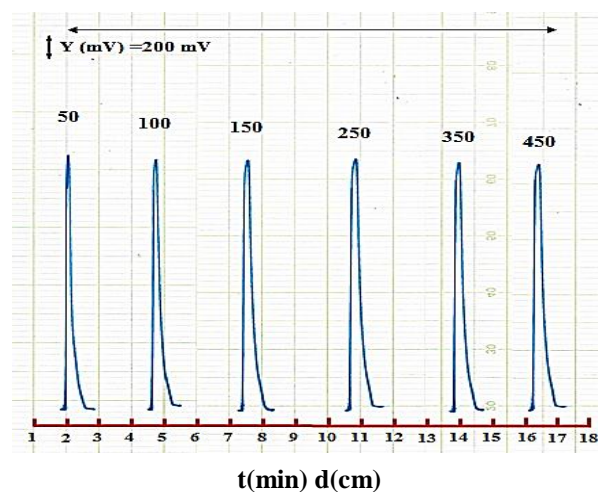

t(min) d(cm)

Figure 5. The effects of various HCl on: A: response profile versus time.

Table 3. A synopsis of the effects of different HCl concentration on the transducer's average responses.

[HCl] mmol/L	Response average $\bar{Y}i$(mV) for(n=3)	RSD%
50	2160	0.1087
100	2140	0.1028
150	2140	0.1074
250	2120	0.1018
350	2100	0.1032
450	2100	0.1047

Physical variables

Flow rate

In order to determine the optimal flow rate. The variation in flow rates between the detector line and the carrier stream within the range (1.0-2.8 ml/min) was studied. The CPM concentration was (4 mmol/L). While maintaining the optimal parameters that were determined in previous written experiments, a peristaltic pump was used to control the flow rate. Fig. 6 shows that bed broadening (increase in analysis time) with a slow flow rate, possibly due to increased dispersion in the flow cell, lengthens the time that the precipitated particles spend facing the detector. When operating at a pump speed faster than 20 (2.0 ml/min for both the detector and the carrier current), a decrease in the intensity of the response was observed. This may be due to how quickly the particles deposited in front of the detector move, i.e. not having enough time for analysis, and this leads to a decrease in the amount of reflected light transmitted. The lower the detector, the lower the peak response. Pump speed 20 (2.0 ml/min) was chosen as the optimal speed in subsequent

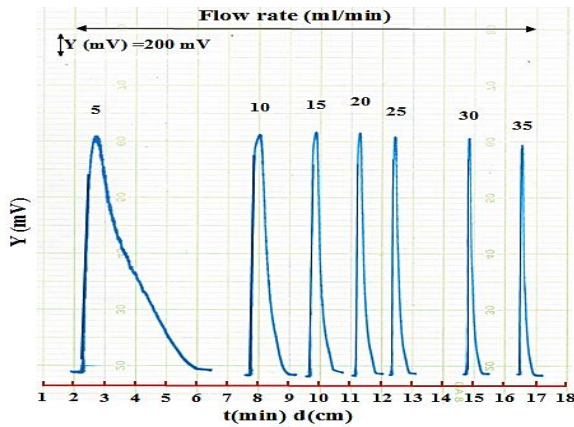experiments because it showed the highest response. The results of the experiment are summarized in Table 4.

Figure 6. The effects of various flow rates on response outline against time.

Table 4. Synopsis of the results of the effect of varying flow rate on the average of transducer's responses.

Pump speed	Flow rate ml/min For both two lines	Response average $\overline{Y}i(mV)$ for(n=3)	RSD%
5	1.0	2100	0.1014
10	1.5	2140	0.1004
15	1.8	2140	0.1018
20	2.0	2160	0.1087
25	2.3	2100	0.1019
30	2.5	2080	0.1009
35	2.8	2060	0.1029

Sample volume
To establish the optimal parameters that were reached in previous experiments and to study the effect of sample volume as one of the physical parameters, different volumes of the injected sample were used within the range (10-100 µl), that is, changing the length of the sample path at the injection valve, in addition to the open valve position (10 sec). The measurement was repeated three times for each sample volume. Figure 7A shows the response profile, from which it was observed that the peaks of the responses increase with increasing

sample volume and at the same time there is also an increase in the width of the base, which means that dispersion increases with increasing sample volume. The sample volume 10 µl showed a higher peak and a smaller base width, so it was chosen as the optimal sample volume in subsequent experiments. The results of the study are summarized in Table 5. Fig. 7B show effect of sample volume on peak rise rate of transducer response and arrival time to the measuring flow cell.
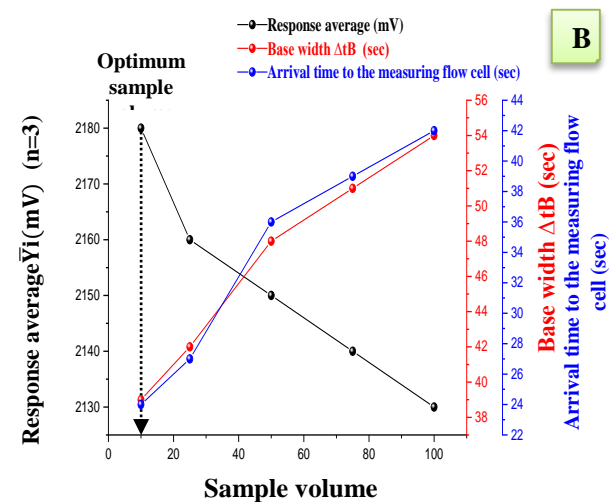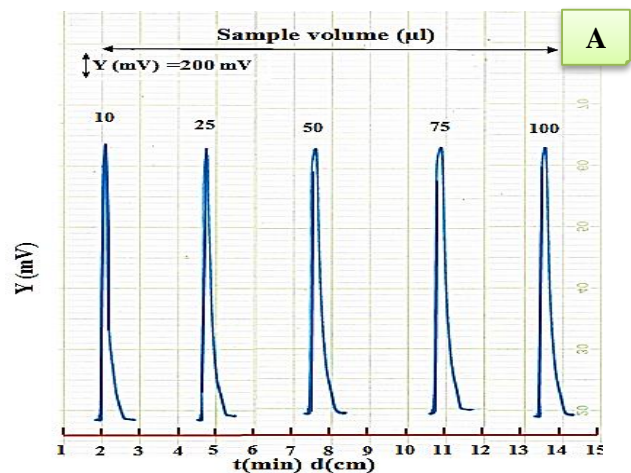

Figure 7. The effects of various sample volume on: A: response outline against time. B: Peak rise rate of transducer response in (mV), base breadth ∆tB (sec) and arrival time to the measuring flow cell (sec).

Table 5. Synopsis of the results of the effect of the difference in the sample volume on the average of transducer's responses.

Sample volume (μl)	Response average $\bar{Y}i$(mV) (n=3)	RSD%	Interval of confidence at (95%),n-1 $\bar{Y}i \pm t_{0.05/2,n-1}.\frac{\sigma_{n-1}}{\sqrt{n}}$	t (sec)	Base breadth ΔtB (sec)	V_{add} (ml) In the flow cell	Concentration mmol//L in the flow cell	Df In flow cell
10	2180	0.1077	2180 ∓5.8381	24	39	2.6100	0.0153	261.4379
25	2160	0.1087	2160 ∓5.8381	27	42	2.8250	0.0354	112.9943
50	2150	0.1009	2150 ± 5.3934	36	48	3.2500	0.0615	65.0406
75	2140	0.1023	2140 ± 5.4407	39	51	3.4750	0.0863	46.3499
100	2130	0.1042	2130 ± 5.5152	42	54	3.7000	0.1081	37.0027

t: Time arrival estimated from the injection valve to the measurement cell (sec), Δt: Base width of peak(sec), V_{add}: Addition volume (ml) in flow cell, Df: Dilution factor in flow cell.

Purge time

Purge time: We mean the time required to completely transfer the sample from the sample loop to the carrier stream. In this experiment, different times were used to purge the sample section (0.4-8 sec), as well as the opening position of the injection valve (10 sec). The carrier solution passes through the injection valve when the valve is in the injection position, next by rotating the valve to the loading position. The experiment was carried out using the optimal parameters that were established in previous experiments. The CPM concentration was (4 mmol/L). The results of the experiment as shown in Table 6. Fig. 8A show the response of the transducer against time, which shows a continuous increase in response with increase purge time up to the time of 10 sec which is the open valve mode. Therefore, it was chosen as the optimal time to completely purify the sample from the sample loop .Fig. 8B showed effect of purge time on peak rise rate of transducer response, base breadth ΔtB and arrival time to the measuring flow cell.
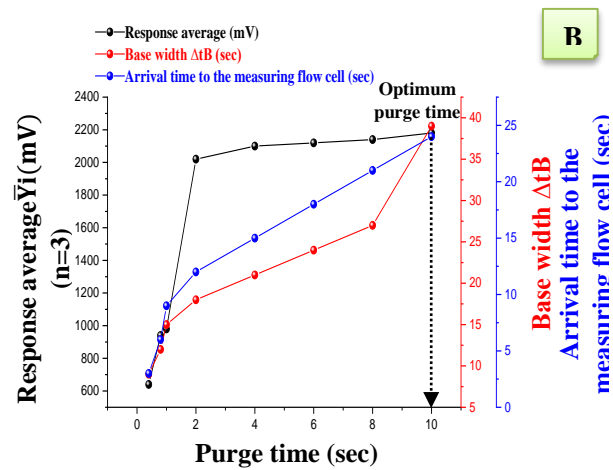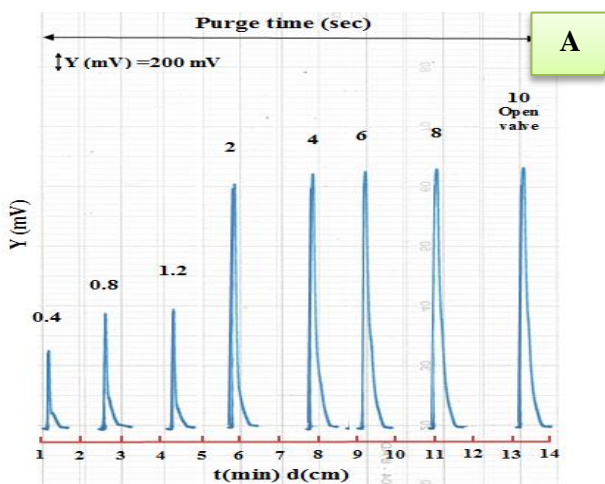

Figure 8. The effects of various purge time on: A: response profile versus time. B: Peak rise rate of transducer's response in (mV)

Table 6. Synopsis of the results of the effect of changing the purge time on the response.

Purge time (sec)	Response average $\bar{Y}i$(mV)for(n=3)	RSD%	t (sec)	Base width ΔtB (sec)
0.4	640	0.1875	3	9
0.8	940	0.1712	6	12
1	980	0.1673	9	15
2	2020	0.1005	12	18
4	2100	0.1009	15	21
6	2120	0.1014	18	24
8	2140	0.1018	21	27
10	2180	0.1077	24	39

Calibration curve (scatter plot) for variance of CPM concentration against transducer response

The optimal chemical and physical parameters were adopted to prepare a series of CPM solutions within the extent (0.07-10) mmol/L; the measurement was repeated for each concentration three successive

times. Responses are shown as in Fig. 9A, which shows the response range and peak height of each concentration of CPM. As shown in the Fig. 9B, the linear calibration curve was within the range (0.07-5) mmol/L, matched by a correlation coefficient(r) =0.9996. The obtained results which briefly show the linear regression of the change of transducer response against the change of CPM concentration, the equation that was used in this part of the study was $\hat{y}=a+bx$ [49] (first degree equation). The value of t was calculated at a confidence level (95%), which was greater than the value of tabular t, which leads us to say that linearity versus nonlinearity is acceptable. The results are summarized in Table 7.
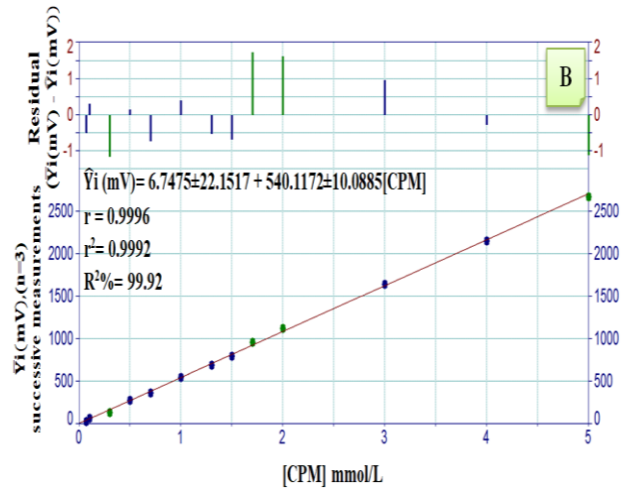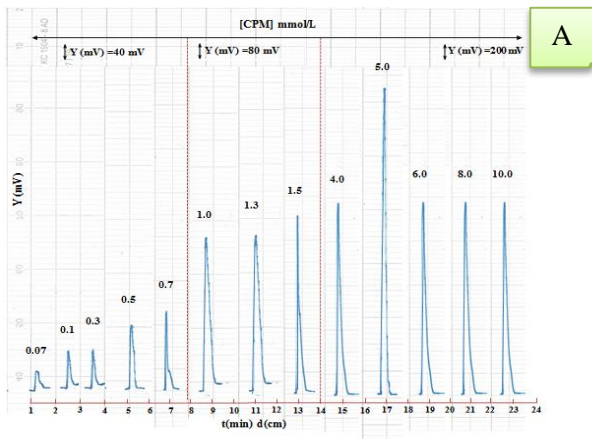
Figure 9. A. Calibration curve for the variation of CPM concentration on response outline versus time B. Linear equation expression of the energy transducer response for new method, $\overline{Y}i$ respons average for three successive measurements

Table 7. Synopsis of results the transducer's response average against changing CPM concentration using first degree equation.

Type of mode	Extent of [CPM] mmol/L	$\hat{Y}(mV) = a\pm sa.t+b\pm sb.t[CPM]$ mmol/L at level of confidence 95%,n-2	r r² R²%
Calibration curve	0.07-10 (n=16)	$395.5215\pm 354.6416+257.9954\pm 87.5265$ [CPM]	0.8605 0.7406 74.06
Linear range	0.07-5.0 (n=13)	$6.7475\pm22.1517+540.1172\pm10.0885$[CPM]	0.9996 0.9992 99.92

n: number of measurement ,$\hat{Y}(mV)$:estimated value of cell in(mV), r:Correlation coefficient, r²: Coefficient of determination, R²%: Explained variation as a percentage / total variation, $t_{tab}= t_{0.05/2,n-2}$

Limit of detection (L.O.D)
Method's detection limit is the minimum possible concentration that the device can sense. A study was conducted to calculate the detection limit for CPM through three methods: practically based on dilute to the minimum concentration gradually, theoretically on the base of the slope value and on the base of linear equation as shown in Table 8. The minimum concentration was (0.07 mmol/L) and the volume of the sample used was 10µl.

Table 8. Method's detection limits value for CPM.

Practically based on the gradual dilution for the minimum concentration (0.07 mmol/L)	Theoretical based on the value of slope X= 3SB/slope for n=13	Based of linear equation $\hat{Y}=Y_b + 3S_b$
195.0 ng/10µl	6.5129 ng/10µl	0.528 µg/10µl

X= limit of detection value, SB=standard deviation value of blank refined for 16 times, Y_b: average response for blank=intercept (a), S_b: Standard

deviation equal to Sy/x(residual) from linear range ,$\hat{Y}$:estimated response(mV).

Repeatability

The measurement of precision achieved by the whole assay process, Fig. 10 and Table 9, sum up measurements of three concentration of CPM (0.1, 1.5 and 4.0) mmol/L. The responses were re-measured for each concentration through eight consecutive injections the relative standard deviation as a percentage was less than 0.2%, makes it abundantly evident that the suggested approach and instrument were suitable for determining CPM.
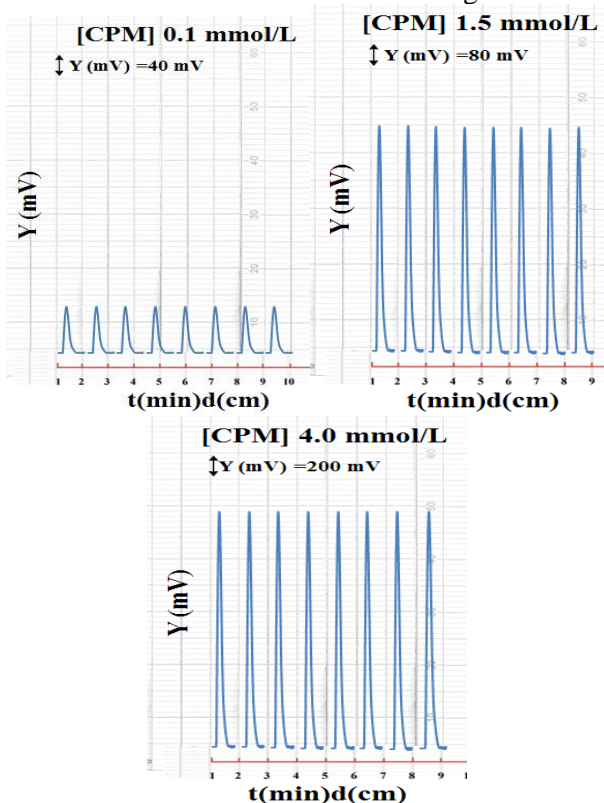

Figure 10. Response outline for eight times of repeated measurement of CPM concentration (0.1, 1.5, 4.0) mmol/L.

Table 9. Synopsis of results for repeatability of CPM at optimal parameters.

[CPM] mmol/L	Response average $\bar{Y}i$(mV) for(n=8)	RSD%
0.1	68	0.1029
1.5	800	0.1125
4.0	2160	0.1018

n= 8, n: number of injection, ttab$0.05_{/2,7}$= 2.365

Classical method of UV-Spectrophotometric

In order to evaluate the new method for estimating CPM, a comparison was made between it and the UV spectrophotometric method, in which CPM was estimated directly without using any detector. The maximum wavelength was determined at 261 nm in Fig. 11A using a quartz cell 1 ml (1000µl), path way was 1cm; the length of the course of the radiation path was 1cm. From Fig. 11B, the calibration curve was within the range (0.001-0.022 mmol/L), while the linear range was (0.001-0.018 mmol/L). Correlation coefficient (r)= 0.9986 and R^2%= 99.72, n= 9 (n= number of measurements). The detection limit was 195.43 ng/1000 µl; it was calculated by gradually diluting the minimum concentration in the calibration curve (0.001 mmol/L). Summary of method results in Table 10.
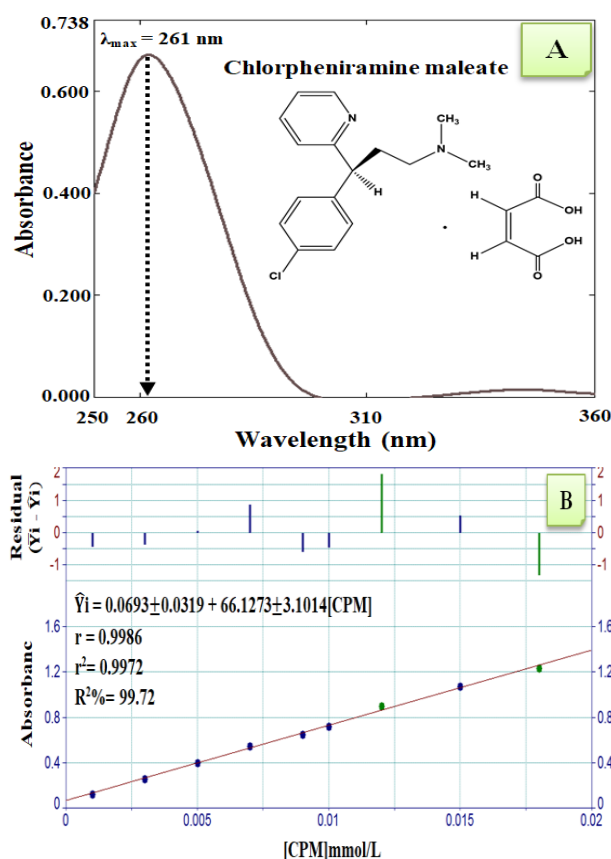

Figure 11.A. Absorbance of UV-Spectrum of CPM at concentration 0.009 mmol/L that shows λ_{max}=261 nm. B. Scatter plot at (0.001-0.022)mmol/L , n=11 for CPM using classical method at 261 nm , in addition to linear range at (0.001-0.018)mmol/L for n=9.

Table 10. Synopsis of linear regressive for the determination of CPM using UV-Spectrophotometric method (classical method).

Type of mode	Extent of calibration curve	Linear regressive at confidence level 95%, n-2 $\hat{Y}=a \pm sat + b \pm sbt$ [CPM]	r r² R²%	L.O.D.
Calibration curve	0.001-0.022 (n=11)	$0.1264 \pm 0.0911 + 57.6491 \pm 7.0486$[CPM]	0.9870 0.9743 97.43	195.43 ng/1000µl
Linear range	0.001-0.018 (n=9)	$0.0693 \pm 0.0319 + 66.1273 \pm 3.1014$[CPM]	0.9986 0.9972 99.72	

n: number of measurement ,$\hat{Y}$(mV):estimated value without unite on spectrophotometric, r: Correlation coefficient, r^2: Coefficient of determination, $R^2\%$: Explained variation as a percentage / total variation, $t_{tab}=t_{0.05/2,n-2}$, L.O.D.: Limit of detection

CPM-ACS-HCl system evaluation for the CFIA method (new method) for determining chlorpheniramine maleate (CPM) in pharmaceutical preparations
To evaluate the efficiency of the new method, which was made using Ayah 6S×1-ST-2D Solar cell CFI analyzer (homemade), to determination CPM in pharmaceutical preparations. Five solutions were prepared for each drug for samples from three different companies for the production of pharmaceutical preparations (SDI-Iraq, Julphar-U.A.E. and Al-Kindi-Iraq), where comparison was made with the UV-Spectrophotometric method (classical method).

Flask number 1 is a sample. Measurements were made for both methods. The results obtained from the standard addition method were mathematically processed. The results are summarized in Tables 11A and B at confidence level (95%). In order to determine whether there is a significant difference or not, both the t-test and F-test were performed, the results were processed statistically [49, 50]. The results of the t-test and F-test were summarized in Table 11B. (column 4 and 5). It was clear from the results that there is no significant difference between the new method and classical method at 95% of the level

of confidence, t-calculated (|-2.162) less than t-tabular (4.303), as well as the calculated F-value (31.9770) less than tabular F-value (39). Fig. 12 shows the effect of variation of CPM concentration on S/N energy transducer response versus time for three samples of drug using Ayah 6SX1-ST-2D solar cell CFI analyzer.
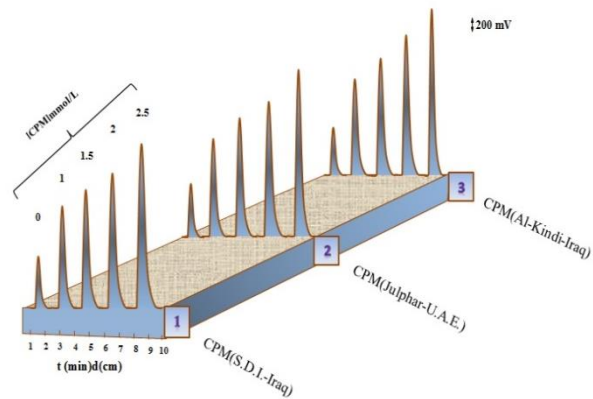

Figure 12. Effect of variation of CPM concentration (using standard addition method) on S/N energy transducer response versus time (min), distains (cm) for three sample drugs using Ayah 6SX1-ST-2D solar cell CFI analyzer. 1-Iraq, Histadin,S.D.I., 2-U.A.E.,Chlorohistol,Julphar , 3-Iraq,Histofen.Al-Kindi

Table 11A. Synopsis of results standard addition in three samples of pharmaceutical preparations for new and classical methods.

Number of sample	Commercial name Company, Content, Country	Type of method						
		New method						
		UV- Sp. method absorbance measurement at λ max=261 nm						
		CPM					standard addition equation at 95% for n-2	r
		0ml	0.5ml	1.5ml	2ml	2.5ml	$\hat{Y}$ (mV)=a mV $\pm$Sa t+ b(Δ y mV /Δxmmol/) bt[CPM]mmol/L	r² R²%
		0	0.5	1.5	2	2.5		

		mmol /L	mmol /L	mmo 1 /L	mmol /L	mmol /L		
		0 ml	0.02ml	0.05 ml	0.07 ml	0.1 ml	$\hat{Y} = a \pm S$ at $+ b$ ($\Delta y / \Delta x$mmol/L)$\pm S$ b t [CPM]mmol/L	
		0	0.002	0.005	0.007	0.01		
1	Histadin S.D.I 4 mg Iraq	570 mV	1210 mV	1460 mV	1760 mV	2055 mV	585.9459±62.7407+589.3243±38.182[CPM] mmol/L	0.9993 0.9987 99.87
		0.410	0.570	0.750	0.910	1.201	0.3987±0.0801+76.9617 ±13.4639 [CPM] mmol/L	0.9954 0.9910 99.10
2	Chlorohistol Julphar 4 mg U.A.E	570 mV	1150 mV	1410 mV	1700 mV	2020 mV	571.8918±49.4590+578.6486±30.0998[CPM] mmol/L	0.9995 0.9991 99.91
		0.400	0.550	0.730	0.900	1.181	0.3847±0.0776+76.5477 ±13.0242[CPM] mmol/L	0.9956 0.9914 99.14
3	Histofen Al-Kindi 4 mg Iraq	570 mV	1150 mV	1410 mV	1700 mV	2020 mV	565.9459±48.6451+574.3243±29.6043[CPM]mmol/L	0.9996 0.9992 99.92
		0.395	0.540	0.733	0.882	1.175	0.3789±0.0773+76.2579 ±12.9873[CPM] mmol/L	0.9956 0.9914 99.14

$\hat{Y}$: Estimated response in (mV) for the new method and the UV-Sp.method absorbance value, r: correlation coefficient, R^2 %: variance explained in percentage /total variation, UV-Sp.: UV-Spectrophotometric method, $t_{tab} = t_{0.05/2,\infty} = 1.960$ at 95%, $t_{tab} = t_{0.05/2,3} = 3.182$ for n=5,using volume of cell (quartz) 1ml in UV-Spectrophotometric method.

Table 11B. Synopsis of practical content results, percentage recovery (Rec. %) for CPM determination in three pharmaceutical preparations, t-test and F-test.

No. of sample	Type of method		Paired t-test		F-test	
	New method					
	UV-Sp.method absorbance measurement at 261 nm					
	Practical concentration (mmol/L) at 10 ml	**Efficiency of determination Rec.%**	$t_{cal} = \frac{\bar{X}d}{\sigma_{n-1}} . \sqrt{n}$	t_{tab} at 95% confidence level	$F_{cal} = S^2_1/S^2_2$	F_{tab}
1	at 10 ml 0.9942 --------------- 9.9420	99.2400				
	0.0051 --------------- 10.3631	103.6026	$\bar{X}d$= -0.0907 σ_{n-1}=0.0737 |-2.162|<	4.303	σ^{**}_{n-1}=0.0158 , $S^2_{1(CFIA)}$=2.5099×10⁻⁴	
2	0.9883 ------------------ 9.8830	98.7200			σ^{*}_{n-1}=0.0895 , $S^2_{2(UVSp.)}$=8.0259×10⁻³	
	0.0050 ----------- 10.0530	100.4953			31.9770 <	39.0000
	0.9854 ------------------	98.4625				

3	9.8540 0.0049 --------------- 9.9389	99.3513

$\overline{X}$d: Comparing two types of methods, on average (new & classical), n(no. of sample)=3, σn-1:standard deviation of different (paired t-test), $t_{tab}=t_{0.05/2,2}=4.303$ (for paired t-test), $F_{tab}= F_{0.95,V1,V2}= F_{0.95,2,2}=39$, σ^{**}_{n-1}: standard deviation for new method, σ^{*}n-1 standard deviation for classical method (F-test),$S^2_{1(CFIA)}$:Variation of new method, $S^2_{2(UV-Sp.)}$:Variation of classical method. UV–Sp.: UV–Spectrophotometric method.

Conclusion

The proposed method was based on studying the precipitate formed by a reaction CPM with ACS in acidic medium using a homemade solar cell analyzer (Ayah 6S×1-ST-2D solar cell-CFI-Analyzer). It was characterized by simplicity and ease of work, not consuming large amounts of sample, reagent, and other materials complementary to the reaction, and the use of a green solvent (distilled water) in all study experiments. The resulting waste was minimal, which makes the method environmentally friendly and meets some of the requirements of green chemistry. The detection limit of the method was in nanograms for a sample volume in microliters. High recovery rates have been obtained from pharmaceutical preparations in which the drug has been estimated.

Acknowledgment

Authors' Declaration

- Conflicts of Interest: None.
- We hereby confirm that all the Figures and Tables in the manuscript are ours. Furthermore, any Figures and images, that are not ours, have been included with the necessary permission for re-publication, which is attached to the manuscript.
- No animal studies are present in the manuscript.
- Authors sign on ethical consideration's approval.
- Ethical clearance: the project was approved by the local ethical committee at University of Baghdad.

Authors' Contribution Statement

M. M. J.and E. N. M. contributed to the design and implementation of the results and to the writing of the manuscript.

References

1. British pharmacopoeia 2020.I. London: The stationery office; 2020. 823. https://www.pharmacopoeia.com/downloads/bp/2020/
2. European pharmacopoeia2019.I. France: Council of Eruope; 2019. 2075.
3. Zeinab A, Marwa M S, Ekram H M, Fatma A F. Assessment of the greenness of micellar HPLC method for rapid separation and simultaneous estimation of chlorpheniramine maleate in presence of some co-administered drugs in three pharmaceutical dosage forms using single run. Acta Chromatogr. 2021; 34(2): 138-149. https://doi.org/10.1556/1326.2021.00883
4. Yulia O S, Vladimir M N, Irina R P, Tatiana A D, Arthur T K, Kristina A M, et al. Food Intolerance:

The Role of Histamine. Nutrients. 2021; 13(9): 1-18. https://doi.org/10.3390/nu13093207

5. Negar D, Reza A. Histamine and Food Allergy. Int J Adv Biol Biomed Res. 2020, 8(2): 100-111. https://doi.org/10.33945/SAMI/IJABBR.2020.2.1

6. Antonio N, María N, Ángel M. The clinical evidence of second-generation H1-antihistamines in the treatment of allergic rhinitis and urticaria in children over 2 years with a special focus on rupatadine. Expert Opin Pharmaco. 2021; 22(4): 511-519. https://doi.org/10.1080/14656566.2020.1830970

7. Martin I, Peter R. Histamine and antihistamines. Anaesth Intensive Care Med. 2021; 22(11):749-755. https://doi.org/10.1016/j.mpaic.2021.07.025

8. Sophia L, Lubnaa H, Anne K. Ellis Evidence-based use of antihistamines for treatment of allergic conditions. Ann Allergy Asthma Immunol. 2023; 131(4): 412-420. https://doi.org/10.1016/j.anai.2023.07.019

9. Liqiao L, Runqiu L, Cong P, Xiang C, Jie L. Pharmacogenomics for the efficacy and side effects of antihistamines. Exp Dermatol. 2022; 31: 993-1004. https://doi.org/10.1111/exd.14602

10. Jawad A, Najaf A, Mazhar I, Shahbaz M, Mohammad Q N. Efficacy of Antihistamine Nasal Spray Compared with Oral Antihistamine in Treatment of Allergic Rhinitis. Pak J Med Health Sci. 2023; 17(4): 539-541. https://doi.org/10.53350/pjmhs2023174539

11. WHO .News release of the 28th November 2017 on falsified medical products. WHO, Geneva.

12. Marcos S, Sayd A R, Joselit T, Gustavo F. A Randomized Controlled Pilot Trial to Test the Efficacy of Intranasal Chlorpheniramine Maleate With Xylitol for the Treatment of Allergic Rhinitis. Cureus. 2021; 13(3): 1-5. https://doi.org/10.7759/cureus.14206

13. Mumin F H, Emad T H, Ali I K. Development of derivative of subtracting spectra method for the simultaneous determination of some decongestant drugs. SJPAS. 2021; 3(3): 18-30. (In Arabic). https://doi.org/10.54153/sjpas.2021.v3i3.264

14. Mayuresh K, Lalit P, Shaheen S, Pramita W. Post-Marketing Surveillance Study to Substantiate the Efficacy and Safety for the Combination of Paracetamol, Phenylephrine, Chlorpheniramine Maleate, Sodium Citrate and Menthol in Indian Patients of Common Cold. Int J Inn Res Med Sci. 2021; 6(7): 430-434. https://doi.org/10.23958/ijirms/vol06-i07/1159

15. Mayuresh K, Lalit P, Pramita W, Shaheen S. Post-marketing surveillance study to evaluate the efficacy and safety for the combination of paracetamol, phenylephrine and chlorpheniramine maleate in paediatric patients of common cold. World J Pharm Res. 2021; 10(8): 1504-1513. http://dx.doi.org/10.32553/ijmsdr.v5i7.820

16. Takemichi F, Asako Y, Atsushi E, Kiyoshi M, Shinichi S, Ayumi Y. Pharmacotherapy of Itch-Antihistamines and Histamine Receptors as G Protein-Coupled Receptors. Int J Mol Sci. 2022; 23(12): 1-12. https://doi.org/10.3390/ijms23126579

17. Ying Z, Xiaoyan Z, Hengxi J, Lu C, Jiang J, Zhongwei Z. Histamine Intolerance-A Kind of Pseudo allergic Reaction. Biomolecules. 2022; 12(3): 1-18. https://doi.org/10.3390/biom12030454

18. Minjae J K, Vishnutheertha K, Micah A G, Torunn E S. Exploring the interactions of antihistamine with retinoic acid receptor beta (RARB) by molecular dynamics simulations and genome-wide meta-analysis. J Mol Graph Model. 2023; 124: 108539. https://doi.org/10.1016/j.jmgm.2023.108539

19. Murugan E, Poongan A, Kesava M. Vinitha A. Synthesis and characterization of graphene nanosheets for electrochemical quantification of chlorpheniramine maleate drugs using a modified glassy carbon electrode. Indian J Chem Technol. 2022; 29:713-720. https://doi.org/10.56042/ijct.v29i6.67423 .

20. Marcos A S, Syed A A, Joselit T, Gustavo F. A Randomized Controlled Pilot Trial to Test the Efficacy of Intranasal Chlorpheniramine Maleate With Xylitol for the Treatment of Allergic Rhinitis. Cureus. 2021; 13(3):1-5. https://doi.org/10.7759/cureus.14206

21. Amrutha D T, Soujanya S. A comparative study of efficacy of fexofenadine with chlorpheniramine maleate in allergic rhinitis in the outpatient department of otorhinolaryngology. Natl J Physiol Pharm Pharmacol. 2021; 11(4): 406-410. https://doi.org/10.5455/njppp.2021.11.11338202016122020

22. Anfal R M, Fanar M A. UV- Spectral Studies on Chlorpheniramine Maleate In Pure Form And Pharmaceutical Preparations. Egypt. J Chem. 2021; 64(8): 4151 - 4156. https://doi.org/10.21608/EJCHEM.2021.31063.2837

23. Linda C D, Nassifatou K. Validation of an UV-Visible spectrophotometry assay method for the determination of chlorpheniramine maleate tablets without prior extraction. Int J Biol Chem Sci. 2021; 15(1): 73-281. https://doi.org/10.4314/ijbcs.v15i1.24

24. Hussein N G, Saeed A M. Simultaneous estimation of chlorpheniramine maleate and glyceryl guaiacolate in pure and capsule dosage form by using different spectrophotometric methods. Res J Pharm Technol. 2021; 14(5): 2608-2612. https://doi.org/10.52711/0974-360X.2021.00459

25. Zeinab A, Marwa M S, Ekram H M, Fatma A F. Assessment of the greenness of micellar HPLC method for rapid separation and simultaneous estimation of chlorpheniramine maleate in presence

of some co-administered drugs in three pharmaceutical dosage forms using single run. Acta Chromatogr. 2021; 34(2): 138-149. https://doi.org/10.1556/1326.2021.00883

26. Hasan A, Thamer A. Omar Development of HPLC Method for Simultaneous Determination of Ibuprofen and Chlorpheniramine Maleate. Sci Pharm. 2022; 90(3): 1-9. https://doi.org/10.3390/scipharm90030053

27. Afsaneh N, Mohamad S T, Samaneh F, Naficeh S. Separation and simultaneous determination of paracetamol, phenylephrine hydrochloride and chlorpheniramine maleate in a commercial tablet by a rapid isocratic HPLC method. Hum Health Halal Metrics. 2020; 2(1): 8-14. https://doi.org/10.30502/JHHHM.2020.224438.1014

28. Madhusudan T B, Sunil V S, Shankar L T. Simultaneous determination of four active pharmaceuticals in tablet dosage form by reversed phase high performance liquid chromatography. Trop J Pharm Res. 2019; 18(10): 2161-2166. https://doi.org/10.4314/tjpr.v18i10.23

29. Ahmed K A, Khalaf F A. Innovation and validation of a new RP-HPLC method for the simultaneous determination of chlorpheniramine maleate, phenylphrine HCl, glycerylguaiacolate, methylparaben, propylparaben and yellow No.6 in pharmaceutical syrup. AIP Conf Proc. 2022; 2394(1): 22-40. https://doi.org/10.1063/5.0121434

30. Amir A ,Umar F, Mahmood A, Muhammad M A, Salman M, Saira A, et al. Stability-Indicating RP-HPLC Assay for Simultaneous Determination of Chlorpheniramine Maleate and Prednisolone in Veterinary Injection. Acta Chromatogr. 2020; 32(2): 122-127. https://doi.org/10.1556/1326.2019.00593

31. Bitar Y. Separation and Assay of Three Anti-Cough Drugs Pseudoephedrine, Dextromethorphan and Chlorpheniramine in Pharmaceutical Forms by using single RP-HPLC Method. Res J Pharm Technol. 2020; 13(2): 831-839. https://doi.org/10.5958/0974-360X.2020.00157.2

32. Muhamad E, Fadi A, Yaser B, Saleh T . Determination of dimenhydrinate and chlorpheniramine maleate in pharmaceutical forms by new gas chromatography method. Res J Pharm Technol. 2019; 12: 2851-2856. https://doi.org/10.5958/0974-360X.2019.00480.3

33. Chunling Y, Yuhai T, Xiaonian H. Flow injection chemiluminescence analysis of diphenhydramine hydrochloride and chlorpheniramine maleate. Instrum Sci Technol. 2006; 34: 529-536. https://doi.org/10.1080/10739140600809421

34. Elham N M, Kawther A S, Tamara A A. A Review Using Continuous FlowInjection Analysis Technique in the Determination of Several Drugs. Ibn Al-Haitham J Pure Appl Sci. 2024; 37(1): 221-235. https://doi.org/10.30526/37.1.3182

35. Jalal N J, Nagham S T. An optoelectronic flow-through detectors for active ingredients determination in the pharmaceutical formulations. J Pharm Biomed Anal 2021; 201: 1-11. https://doi.org/10.1016/j.jpba.2021.114128

36. Ghadah F H, Nagham S T. A new continuous flow injection analysis method with NAG-ADF-300-2 Analyzer for promethazine-HCl by cadmium iodide as a precipitating reagent. Chem Methodol. 2021; 5: 498-512. https://doi.org/10.22034/chemm.2021.138807

37. Nagham S T, Elham N M. Assessment of long distance chasing photometer (NAG-ADF-300-2) by estimating the drug atenolol with ammonium molybdate via continuous flow injection analysis. Baghdad Sci J. 2020; 17(1): 78-92. https://doi.org/10.21123/bsj.2020.17.1.0078

38. Elham N.M, Nagham S T. Assessment of long distance chasing photometer (NAG-ADF-300-2) by estimating the drug Atenolol with povidone iodine via CFIA. Ibn Al-Haitham J Pure Appl Sci. 2020; 33(1): 65-83. https://doi.org/10.30526/33.1.2383

39. Raed F H. New mode semi-automated turbidimetric determination of mefenamic acid by Ayah 6SX1-ST-2D solar cell-CFI analyser. Res J Pharm Technol. 2019; 12(12): 5773-5780. https://doi.org/10.5958/0974-360X.2019.00999.5

40. Nagam S T, Kefah H I. Turbidimetric determination of metoclopramide hydrochloride in pharmaceutical preparation via the use of a new homemade Ayah 6SX1-T-2D solar cell-continuous flow injection analyser. Iraqi J Sci. 2015; 56(2B): 1224-1240.

41. Nagam S T, Mustafa K K. Determination of mfenamic acid using a new mode of irradiation (Ayah of six identical leds) and detection (twin solar cells) through turbidity measurement by CFIA. Iraqi J Sci. 2016; 57(23): 1052-1070.

42. Muntadhar M J, Elham N M. Fast New Method for Estimation of Captopril in Pure and Pharmaceutical Preparation by Reaction with Ammonium Ce (IV) Sulfate in Acid Medium. Ibn Al-Haitham J Pure Appl Sci. 2024; 37(1): 265-282. https://doi.org/10.30526/37.1.3191

43. Nagam S T, Omar A Y. New Method for Estimation Mebeverine Hydrochloride Drugs Preparation by a New Analyser: Ayah 6S.X1(WSLEDs)-T.- Two Solar Cells Complied with C.F.I.A. Baghdad Sci J. 2021; 18(3): 565-574. http://dx.doi.org/10.21123/bsj.2021.18.3.0565

44. Nagam S T, Rana A K. CFIA turbidimetric and photometric determination of vitamin B_9 (Folic acid) using leds as a source of irradiation and two solar cell as an energy transducer .Baghdad Sci J. 2017; 14(4): 773-786. https://doi.org/10.21123/bsj.2017.14.4.0773

45. Muntadhar M J, Elham N M. Continuous Flow Injection Analysis Method for the Determination of a Drug Diphenhydramine Hydrochloride by Using

Phosphomolybdic Acid. Baghdad Sci J. 2024; 8 Online. https://dx.doi.org/10.21123/bsj.2024.8926

46. Paul A, Nicolas E. Green Chemistry: Principles and Practice. Chem Soc Rev.2010; 39: 301-312. https://doi.org/10.1039/B918763B

47. Nagaraj S, Deepti N. Electrochemical detection of chlorpheniramine maleate in the presence of an anionic surfactant and its analytical applications. Can J Chem. 2017; 95(5): 1-23. https://doi.org/10.1139/cjc-2016-0406

48. Nagam S T, Issam M. A, Kefah H I. Novel Study of Cyproheptadine Hydrochloride Precipitate Formed by Potassium hexacyanoferrate and Sodium nitroprusside using Atomic Force Microscopy. Iraqi J Sci. 2015; 56(4A): 2745-2761.

49. Miler J C, Miler J.N. Statistics for analytical chemistry .6th ed. 2010; St. John Wiley and N.Y. Sons.

50. Murdoch J.; Barnes J.A. Statistical tabltes.4th Ed. 1998, Macmillan.

تقدير مادة الكلورفينيرامين ماليات في مستحضراتها الصيدلانية باستخدام محلل الحقن الجرياني العكر محلي الصنع

منتظر محمد جبار، الهام نغيمش مزعل

قسم الكيمياء، كلية التربية للعلوم الصرفة (ابن الهيثم)، جامعة بغداد، بغداد، العراق.

الخلاصة

باستخدام تقنية التحليل بالحقن الجرياني المستمر: تم في هذه الدراسة تقديم طريقة تحليلية جديدة لتقدير مادة الكلورفينيرامين ماليات (CPM) في صورتها النقية وفي بعض مستحضراتها الصيدلانية. اعتمدت الدراسة على تفاعل CPM مع كبريتات الأمونيوم السيريوم الرباعي (ACS) في وسط حمضي، حيث نتج عن التفاعل راسب أبيض مصفر قليلاً. تمت دراسة الراسب المتكون باستخدام محلل الخلايا الشمسية محلي الصنع (Ayah 6SX1-ST-2D solar cell CFI analyzer) عن طريق قياس الضوء المنعكس من سطوح دقائق الراسب عند (0-180 درجة). تم إجراء بعض التجارب لدراسة وتحسين بعض المعلمات الكيميائية والفيزيائية. كان معامل الارتباط (r) = 0.9996، و منحنى المعايرة الخطية ضمن المدى (0.07-5 ملمول/لتر). حد الكشف للطريقة المقترحة (L.O.D) هو 195 نانوغرام/10 ميكرولتر. كانت نسبة الانحراف النسبي RSD% أقل من 0.2% للتراكيز 0و1، 0و5 و0و4 مليمول/لتر من CPM تم تكرار القياس لكل تركيز 8 مرات. تم تطبيق الطريقة بنجاح في تقدير CPM في ثلاث عينات من المستحضرات الصيدلانية المتوفرة في سوق الأدوية العراقي لثلاث شركات مختلفة. تمت مقارنة الطريقة الجديدة مع طريقة قياس الطيف الضوئي للأشعة فوق البنفسجية عند طول موجي اعظم 261 نانومتر. وللتأكد من عدم وجود فرق معنوي مهم بين الطريقة المقترحة وطريقة القياس الطيفي، تم إجراء اختبار t واختبار F. وأظهرت نتائج الاختبارين عدم وجود فروق معنوية عند مستوى ثقة 95%، حيث كانت قيمة t المحسوبة 162و2. وهي أقل من قيمة t الجدولية (4.303) وكذلك قيمة F المحسوبة (31.9770) أقل من قيمة F الجدولية.

الكلمات المفتاحية: مضادات الهستامين، كلوروفينيرامين ماليات، محلل CFI ، الحقن الجرياني المستمر، دقائق الراسب، طريقة قياس الطيف الضوئي للأشعة المرئية و فوق البنفسجية